



# Explainable artificial intelligence (XAI) for interpreting the contributing factors feed into the wildfire susceptibility prediction model

Abolfazl Abdollahi<sup>a,b,\*</sup>, Biswajeet Pradhan<sup>b,c,\*\*</sup>

<sup>a</sup> Fenner School of Environment & Society, College of Science, The Australian National University, Canberra, ACT, Australia

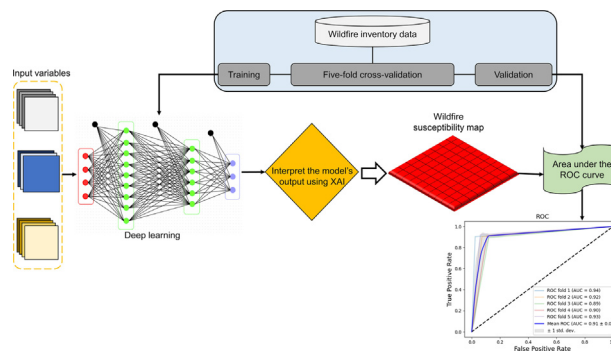
<sup>b</sup> Centre for Advanced Modelling and Geospatial Information Systems, School of Civil and Environmental Engineering, Faculty of Engineering and IT, University of Technology Sydney, Ultimo, NSW 2007, Australia

<sup>c</sup> Earth Observation Centre, Institute of Climate Change, Universiti Kebangsaan Malaysia, 43600 UKM Bangi, Selangor, Malaysia

## HIGHLIGHTS

- Wildfire susceptibility prediction using deep learning for Gippsland, Victoria
- Understanding the effect of conditioning factors towards wildfire occurrence
- Explainable artificial intelligence (XAI) is utilized to interpret the prediction results.
- Cross-validation is used for a more accurate model performance assessment.

## GRAPHICAL ABSTRACT



## ARTICLE INFO

Editor: Fernando A.L. Pacheco

**Keywords:**  
Wildfire susceptibility  
Deep learning  
Machine learning  
SHAP  
XAI  
GIS

## ABSTRACT

One of the worst environmental catastrophes that endanger the Australian community is wildfire. To lessen potential fire threats, it is helpful to recognize fire occurrence patterns and identify fire susceptibility in wildfire-prone regions. The use of machine learning (ML) algorithms is acknowledged as one of the most well-known methods for addressing non-linear issues like wildfire hazards. It has always been difficult to analyze these multivariate environmental disasters because modeling can be influenced by a variety of sources of uncertainty, including the quantity and quality of training procedures and input variables. Moreover, although ML techniques show promise in this field, they are unstable for a number of reasons, including the usage of irrelevant descriptor characteristics when developing the models. Explainable AI (XAI) can assist us in acquiring insights into these constraints and, consequently, modifying the modeling approach and training data necessary. In this research, we describe how a Shapley additive explanations (SHAP) model can be utilized to interpret the results of a deep learning (DL) model that is developed for wildfire susceptibility prediction. Different contributing factors such as topographical, landcover/vegetation, and meteorological factors are fed into the model and various SHAP plots are used to identify which parameters are impacting the prediction model, their relative importance, and the reasoning behind specific decisions. The findings drawn from SHAP plots show the significant contributions made by factors such as humidity, wind speed, rainfall, elevation, slope, and normalized difference moisture index (NDMI) to the suggested model's output for wildfire susceptibility mapping. We infer that developing an explainable model would aid in comprehending the model's decision to map wildfire susceptibility, pinpoint high-contributing components in the prediction model, and consequently control fire hazards effectively.

\* Correspondence to: A. Abdollahi, Fenner School of Environment & Society, College of Science, The Australian National University, Canberra, ACT, Australia.

\*\* Correspondence to: B. Pradhan, Centre for Advanced Modelling and Geospatial Information Systems, School of Civil and Environmental Engineering, Faculty of Engineering and IT, University of Technology Sydney, Ultimo, NSW 2007, Australia.

E-mail addresses: [Abolfazl.Abdollahi@anu.edu.au](mailto:Abolfazl.Abdollahi@anu.edu.au) (A. Abdollahi), [biswajeet.pradhan@uts.edu.au](mailto:biswajeet.pradhan@uts.edu.au) (B. Pradhan).

<http://dx.doi.org/10.1016/j.scitotenv.2023.163004>

Received 24 January 2023; Received in revised form 2 March 2023; Accepted 18 March 2023

Available online 24 March 2023

0048-9697/© 2023 The Authors. Published by Elsevier B.V. This is an open access article under the CC BY-NC license (<http://creativecommons.org/licenses/by-nc/4.0/>).

## 1. Introduction

Wildfires have been one of the biggest and most prevalent threats harming natural ecosystems in recent decades. Globally, fires decimate millions of hectares of rangelands and forests each year (Zhongming et al., 2020). Natural fires can occur in rangelands and forests due to a variety of variables, including friction between dry litter, litter accumulation, lightning, insufficient precipitation, global warming, deforestation, hot winds, climate change, and poor land management (Chuvieco et al., 2003; Ganteaume et al., 2013). Over time, wildfires have become more frequent, and the damage caused by wildfires to forests worldwide is estimated at 37 million ha each year (Ajin et al., 2015). In addition to seriously damaging infrastructure and human life, wildfires have caused major destruction to ecosystems (Sayad et al., 2019). By detecting places that are highly fire susceptible, applying fire prevention, and taking fire safety precautions, damage caused by fire can be reduced (Jaiswal et al., 2002). Determining the elements that influence the incidence of fire, such as human activities, topographic, climatic, and fuel conditions is necessary in order to identify fire-susceptible zones (Vasilakos et al., 2009). As a result, it is necessary to establish the connection between these elements and the likelihood of fire (Naderpour et al., 2021). To accomplish this, it is required to keep track of places by establishing good quality fire-inventory where past fires have happened and then compares those locations to layers of the elements impacting fire susceptibility to ascertain how they are related (Smith and Lyon, 2000).

A multi-scaled system of wildfire parameters, including climate (e.g., rainfall, temperature, wind speed, humidity, etc.), topography (e.g., elevation, slope, aspect), and landcover and vegetation factors are used as the predicting variables in the modeling and mapping of wildfire susceptibility (Iban and Sekertekin, 2022). Globally, wildfire susceptibility has been mapped by several research (Gholamnia et al., 2020; Pradhan et al., 2007; Tien Bui et al., 2016). For predicting and simulating the wildfire likelihood spatial pattern in various geographical areas, a variety of spatial modeling techniques have been developed with different predicting variables (Talukdar et al., 2022). Some of these researches combined remote sensing derived data and geographic information systems (GIS) data with multi-criteria decision analysis (MCDA) to estimate the susceptibility of wildfires. For example, Nami et al. (2018) applied the evidential belief function (EBF) method using 1162 wildfire points and 14 predicting variables for wildfire susceptibility mapping in the Hyrcanian ecoregion, northern Iran. The findings demonstrated the GIS-based EBF model's efficacy in wildfire probability prediction with the values of 84.14 % for the area under curve (AUC). In order to assess the significance of each wildfire conditioning element and identify high-risk wildfire zones in Iran's Mazandaran Province, Eskandari and Miesel (2017) employed a knowledge-based analytical hierarchical process (AHP) and fuzzy sets. The findings demonstrated the capability of the fuzzy AHP method to identify high-risk locations for fire in Iran's Hyrcanian forests. The spatial distribution of natural disasters like wildfires has also been widely analyzed and predicted using machine learning (ML) models such as random forest (RF) (Kim et al., 2019), neural networks (NNs) (Dutta et al., 2016), logistic regression (Kuter et al., 2011), and support vector machine (SVM) (Al-Fugara et al., 2021). The development of ML algorithms depends on the training data availability, and different ML techniques have different advantages and disadvantages (Tavakkoli Pirailou et al., 2022). In particular, in the mapping of natural hazards susceptibility, ML models have demonstrated their ability to effectively handle non-linearity issues in spatial simulation, modeling, and mapping (Eskandari et al., 2021). Moreover, compared to traditional methods like MCDA, the key benefit of merging ML algorithms with GIS approaches is typically a better performance of the resulting wildfires prediction as well as a faster rate of data processing (Jaafari et al., 2019). Several statistical and ML models, such as NN, RF, SVM, decision tree, radial basis function, least angle regression and logistic regression, were assessed in a comprehensive wildfire susceptibility study (Gholamnia et al., 2020). The accuracy evaluation of the study showed that RF represents the wildfire prediction with the best accuracy, with an

area under the curve (AUC) of 88 %, followed by SVM with a 79 % AUC. To assess the locations of forest fires in South Korea, Kim et al. (2019) used two ML models such as RF and maximal entropy. Their research showed that this wildfire hazard had a significant link with human-related factors and the highest wildfire probabilities were found in the vicinity of settlement regions. Three ML models, including multivariate adaptive regression splines, SVM, and boosted regression tree were applied by (Kalantar et al., 2020) for the wildfire susceptibility mapping using 14 critical indicators that influence wildfires. In recent years, the state-of-the-art machine learning technique such as deep learning models (DLs) has also gained popularity in the remote sensing field, especially in wildfire susceptibility and risk predictions (Naderpour et al., 2021). Bjānes et al. (2021) implemented an ensemble method based on two DL models to map wildfire susceptibility in two regions in Chile. In order to provide a dataset from which to extract the samples for the models' training, satellite data for 15 fire-influencing elements in the study area was acquired. The results showed that the proposed model achieved the highest accuracy with AUC of 95.3 % in the predicted susceptibility maps. In a recent work, Naderpour et al. (2021) applied a DL model for wildfire susceptibility and risk assessment in the Northern Beaches region of Sydney, Australia. As input to their model, 36 critical key variables influencing the risk of forest fires were chosen and spatially mapped from a variety of contexts, including physical, social, human-induced, climate, morphology, and topography viewpoints. The final outcomes demonstrated the developed model's high level of precision in determining forest fire susceptibility.

The lack of trust, explainability and transparency when utilizing any machine learning model in real-world scenarios is a barrier for wildfire management planners as these algorithms are viewed as being "black box" models, meaning that it is difficult to understand how they arrive at their conclusions. This is because these models are trained on massive amounts of data and make use of complex algorithms that are difficult to interpret (Abdollahi and Pradhan, 2021; Cheng et al., 2021; Maddy and Boukabara, 2021). It has been found in the literature that researchers and decision-makers tend to mostly utilize ML techniques to assess and spatially map wildfire susceptibility. However, the explanation and interpretation of the model outcomes are crucial. Explainable artificial intelligence (XAI) refers to the development of artificial intelligence (AI) systems that can be easily understood and explained by humans (Maddy and Boukabara, 2021). XAI aims to address black box issue by developing AI models that are more transparent and interpretable (Arrieta et al., 2020; Cilli et al., 2022). This can involve using simpler algorithms or designing models in such a way that their internal workings are easier to understand. Additionally, XAI can involve developing tools that allow users to visualize and interact with the model, helping them to understand how it is making decisions (Arrieta et al., 2020). There are many potential benefits to XAI. For example, it can help to build trust in AI models and ensure that they are being used fairly and ethically. It can also help to identify and correct biases in AI systems and models. The introduction of explicable algorithms, such as SHapley Additive exPlanations (SHAP), can influence perceptions of utilizing machine learning (ML) based models for decision-making by making it easier to understand model outputs (Cheng et al., 2021). Therefore, this work's originality lies in implementing an explainable deep learning approach to map wildfire susceptibility and determine which parameters among the meteorological, topographic, and landcover/vegetation factors are influencing the prediction model and their relative importance, the relationships between features, and the reasoning behind specific decisions. This paper attempts to explain how a deep learning method produces a certain result in wildfire prediction of the Gippsland region in Victoria, Australia. This has never been undertaken before in the literature and this is for the first time the proposed model has been implemented. Hence, the current work additionally attempts to interpret model outputs using various SHAP plots. In short, the main objectives of the work are: i) the development of spatial DL framework to map wildfire susceptibility; ii) understanding the model-predictor relationship for various input variables by analyzing the individual predictions using Shapley outputs; iii) considering cross-validation for a more accurate model

performance evaluation and iv) investigating the spatial variation of model results on wildfire susceptibility prediction for the study area. Wildfires across Australia pose a significant hazard each year. It is crucial to focus more on Australia's forest fires risk management strategy to confront this catastrophe due to the rise in the number of fires. As a result, it is imperative to develop an effective and trustworthy framework, such as an explainable machine learning model, which will help the decision-makers to better comprehend model outputs and identify which parameters are showing high contribution and impacting the prediction model, and accordingly better control fires hazard.

## 2. Wildfire susceptibility prediction framework

In this work, we established a methodology for producing a wildfire susceptibility map, which is shown in Fig. 1. The framework's initial phase is to establish 11 contributing elements in relation to the analysis of wildfire susceptibility. Then, we developed a deep learning (DL) method and fed the input parameters into the model to train and test the model based on contributing factors and the wildfire inventory dataset. In the next step, we applied an explainable artificial intelligence (XAI) model to interpret the output of the DL model and check the contribution of each input factor to the prediction. To test the outcome's stability, the model runs for five-fold cross-validation. Finally, the wildfire susceptibility for the study area was spatially mapped, and the performance of the model was assessed and visualized using receiver operating characteristic (ROC).

### 2.1. Study area and inventory data

The Gippsland region in the state of Victoria, Australia, is characterized by various distinctive regions and covers all of southeast Victoria with an area of 41,556 km<sup>2</sup> from 147.46°E to -37.58°S, encompassing bushlands, lakes, farmlands, mountains, and beaches. The Gippsland region has experienced several wildfires over the years and is one of the most bushfire-prone areas. For example, in the 2019–2020 Australian bushfire that is known as “Black Summer”, there were megafires in most parts of Australia, and Gippsland had experienced drought conditions for more than three years by the beginning of the 2019–2020 fire season. The East Gippsland fires resulted in the deaths of four people and the destruction of hundreds of houses, and the evacuation of over a thousand people. The location of the research area in the state of Victoria, Australia, is depicted in Fig. 2.

For obtaining the wildfire inventory map and pinpointing the locations of wildfires for our investigation, we used the moderate resolution imaging spectroradiometer (MODIS) fire and thermal anomalies data such as MCD64A1 and MOD14/MYD14 and historical records (<https://datasets.seed.nsw.gov.au/dataset/fire-history-wildfires-and-prescribed-burns-1e8b6>) from 2019 to 2020. Wildfire ignition is typically influenced by seasonal characteristics. The most likely times for wildfires to occur in Australia are during the summer and spring seasons, extending from October to May. All Australian states witnessed one of the worst forest fires in November 2019, which was primarily caused by severe weather conditions. The training samples in this experiment were labelled at 521 wildfire locations. Using two sets of inventory values of 0 and 1, where 1 indicates the presence of a fire event and 0 indicates the absence of a fire event, the susceptibility model was trained.

### 2.2. Wildfire contributing factors

Several environmental elements, such as man-made features, fuel characteristics, topography, weather and climatic variables, and vegetation types, are linked to the degree of environmental loss caused by wildfires (Naderpour et al., 2021). These elements, which are usually referred to as contributing parameters (Eskandari and Khoshnevis, 2020), have an impact on the size and intensity of wildfires. In this work, 11 significant parameters from three categories (e.g., meteorological, topographic, and landcover/vegetation factors) for the year 2020 are considered to assess their correlation with the wildfire susceptibility prediction in the study area, which is described in detail below.

**Topographical factors:** These factors influence the climatic conditions, notably the rainfall and temperature spatial distribution, which regulate the life cycles of fauna and flora (Tavakkoli Piralilou et al., 2022). The main topographical factors used in this study are aspect, slope, and elevation. The digital elevation model (DEM) serves as the reference map for extracting topographical elements, which was generated from the shuttle radar topography mission (SRTM) with an approximate resolution of 30 m (USGS/SRTMGL1\_003).

**Landcover/vegetation factors:** Fire incidence is significantly influenced by land cover and vegetation types (Ljubomir et al., 2019). We generated some vegetation indices such as green normalized difference vegetation index (GNDVI), normalized difference moisture index (NDMI), and normalized difference vegetation index (NDVI) using Sentinel-2 data with 20 m spatial resolution. With the exception of measuring the green spectrum

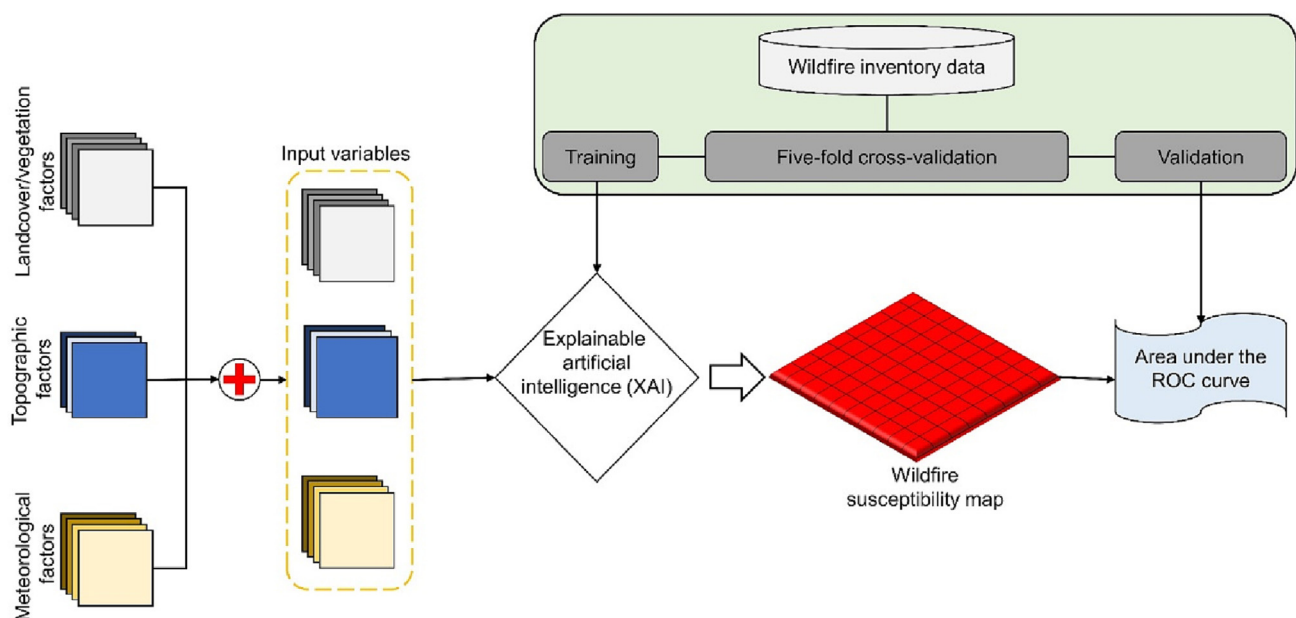


Fig. 1. The suggested deep learning based XAI framework for wildfire susceptibility mapping.

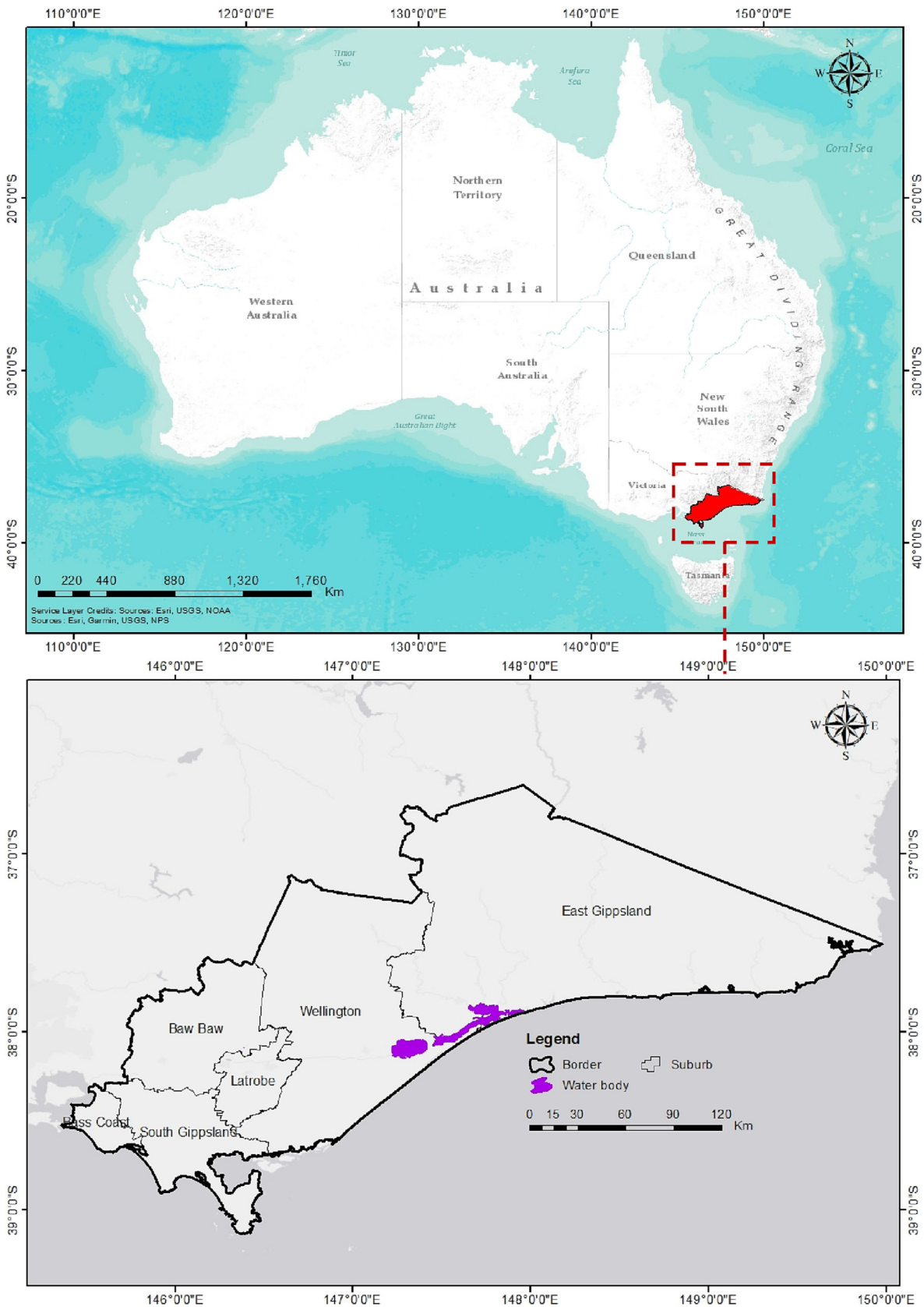


Fig. 2. The location of research area, Gippsland in Victoria state, Australia.

rather than the red spectrum, GNDVI is comparable to NDVI. It measures the photosynthetic activity of the vegetation cover and is frequently used to determine the nitrogen concentration and moisture content of plant

leaves (Navarro et al., 2017). NDMI uses a combination of short-wave infrared (SWIR) and near-infrared (NIR) spectral bands to identify the moisture content of vegetation, which has a profound effect on fire occurrence (Adab

et al., 2013). For the landcover map, we also used ESRI 2020 global land cover from Sentinel-2 product with ten different classes (<https://gee-community-catalog.org/projects/esrilc2020/>) and resampled it to the same as that of Sentinel-2 vegetation indices.

**Meteorological factors:** These factors include rainfall, temperature, humidity, and wind speed. Wind not only blows sparks and flames into fresh fuel but also dries out the soil and surface moisture (Naderpour et al., 2021). The forest surface fuels may be more susceptible to fire ignition in the presence of lower rainfall and relative humidity, and warmer temperatures. Fires can start and spread quickly when windy, dry, and hot conditions are present at the same time (Naderpour et al., 2021). The wind speed factor was obtained from the wind global atlas dataset (<https://gee-community-catalog.org/projects/gwa/>), while the other meteorological parameters were collected from Australian climate datasets (<https://www.longpaddock.qld.gov.au/silo/point-data/>). All the factors were resampled to the same resolution as Sentinel-2 vegetation indices. Table 1 summarizes the list of contributing factors for wildfire susceptibility mapping, and Fig. 3 depicts these layers, which are spatially mapped for the study area.

### 2.3. The architecture of the presented model

As depicted in Fig. 4, the applied deep learning (DL) approach comprises a number of fully connected layers that categorize each contributing factor as an input layer to produce the wildfire susceptibility prediction map. When the input parameters are fed into the DL, the output values are computed sequentially along with the network layers. The input vector, which also contains each unit's output values from the previous layer, is multiplied by the weight vector for each unit in the current hidden layer to create the weighted sum at each layer. The fundamental DL architecture is created by an input layer  $L_x$ , an output layer  $L_y$ , and dense layers  $H$  between the input and output layers  $L_h (h \in \{1, 2, \dots, H\})$ . Each dense layer  $L_h$  comprises a group of units that can be organized into a vector  $a_h \in R^{|L_h|}$ , with  $|L_h|$  signifying the number of units in  $L_h$ . Then, each dense layer  $L_h$  can be parameterized using an activation function  $f()$ , a weight matrix  $W_h \in R^{|L_{h+1}| \times |L_h|}$ , and a bias vector  $b_h \in R^{|L_{h+1}|}$ .  $a_h = f(W_h^T a_{h-1} + b_h)$  can be used to compute the units in  $L_h$ , where  $h = 1, 2, \dots, H$ ,  $L_0$  denotes a compound's features vector, and  $a_0$  denotes the units in the input layer. After performing calculations  $a_H$  for the last dense layer, the Sigmoid function was applied to the output layer  $L_y$  to estimate class probabilities. Additionally, we employed an activation function called the rectified linear unit (ReLU) due to the back-propagation training's sparsity property, lack of gradient vanishing influence, and high processing efficiency (Abdollahi et al., 2022; Glorot et al., 2011), which can be derived as:

$$f(x) = \max(0, x) \tag{1}$$

**Table 1**

An overview of the chosen conditioning elements and their significance in predicting wildfire susceptibility.

Contributing factor	Source	Importance	References
Rainfall	Meteorological data	This element regulates the vegetation moisture and pattern, both of which affect how quickly fires spread.	(Tien Bui et al., 2016)
Wind speed	Wind global atlas	This factor usually causes the fire to spread faster and more dangerously in the direction of the wind.	(Shakesby, 2011)
Temperature	Meteorological data	Radiant heat.	(Verde and Zêzere, 2010)
Humidity	Meteorological data	It has an impact on the fuel moisture content, which then impacts its flammability.	(Won et al., 2006)
Landcover	ESRI land cover	The distribution and risk of wildfires are impacted differently by various landcover patterns.	(Molina et al., 2019)
NDVI	Sentinel-2	It gauges the area's greenness and enables visualization of the condition of the vegetation.	(Eskandari et al., 2021)
GNDVI	Sentinel-2	It serves as a measure of photosynthetic activity and is frequently employed to determine the levels of fuel nitrogen and moisture.	(Navarro et al., 2017)
NDMI	Sentinel-2	This factor identifies the moisture content of vegetation.	(Adeb et al., 2013)
Elevation	SRTM	It is a crucial component in regional climate variability.	(Jaafari and Pourghasemi, 2019)
Slope	SRTM	Both biodiversity and the distribution of vegetation are influenced by this factor.	(Ljubomir et al., 2019)
Aspect	SRTM	In mountainous places, wildfire spreads more quickly on slopes that face east and receive more sun energy.	(González et al., 2018)

The presented method's structure is built on a multilayer feed-forward neural network with the following layer structure: i) the input layer, including the contributing factors fed to the model; ii) there are five dense layers with 100 neurons in each with activation function and dropout between them to avoid saturation and over-fitting problems during the learning process; and iii) Sigmoid classifier was added in the final layer to predict the proper class based on the collection of obtained features from the prior layers. We implemented the full procedure of the model for wildfire susceptibility prediction using Keras with Tensorflow as a backend.

### 2.4. SHapley Additive exPlanations (SHAP) method

A game-theoretic method for assessing the effectiveness of the prediction algorithm is called SHAP (Chen, 2021). In order to provide an understandable method, SHAP uses an additive feature imputation methodology, in which the model's output is stated as a linear addition of input variables. In supervised settings, SHAP's robust theoretical foundation is advantageous. It describes a specific prediction using Shapley values by assigning a SHAP value to any factor that satisfies the following requirements (Mangalathu et al., 2020): 1) local accuracy - the explanation approach must at least match the results of the main model; 2) missingness - features that are absent in the main input need to be disregarded; 3) consistency - the significance of a variable should not drop if we alter a model to make it more dependent on that variable, regardless of how relevant other variables are. As a result, SHAP can effectively describe both global and local procedures. A local model uses the most basic background information from the data to create an interpretable method that considers the proximity to the instance (Ribeiro et al., 2016). The SHAP structure compiles explanation strategies like LIME (Ribeiro et al., 2016) and DeepLIFT (Shrikumar et al., 2017) into the area of additive feature attribution procedures. For the main approach  $f(x)$  with input variables  $x = (x_1, x_2, \dots, x_p)$  that  $p$  is the number of input variables, the explanation method  $g(x')$  with streamlined input  $x'$  can be calculated as:

$$f(x) = g(x') = \phi_0 + \sum_{i=1}^M \phi_i x'_i \tag{2}$$

where,  $M$  is the number of input features, and  $\phi_0$  is the consistent value.

To approximate SHAP values, there are several methods, including Kernel SHAP, Deep SHAP, and Tree SHAP (Lundberg and Lee, 2017). Using Shapley values and linear LIME, kernel SHAP, a model-agnostic estimator, creates a local explanatory method (Ribeiro et al., 2016). Kernel SHAP was employed in this work because, when compared to other sampling-based estimates, it provides more accurate estimations with lower model evaluations (Abdollahi and Pradhan, 2021).

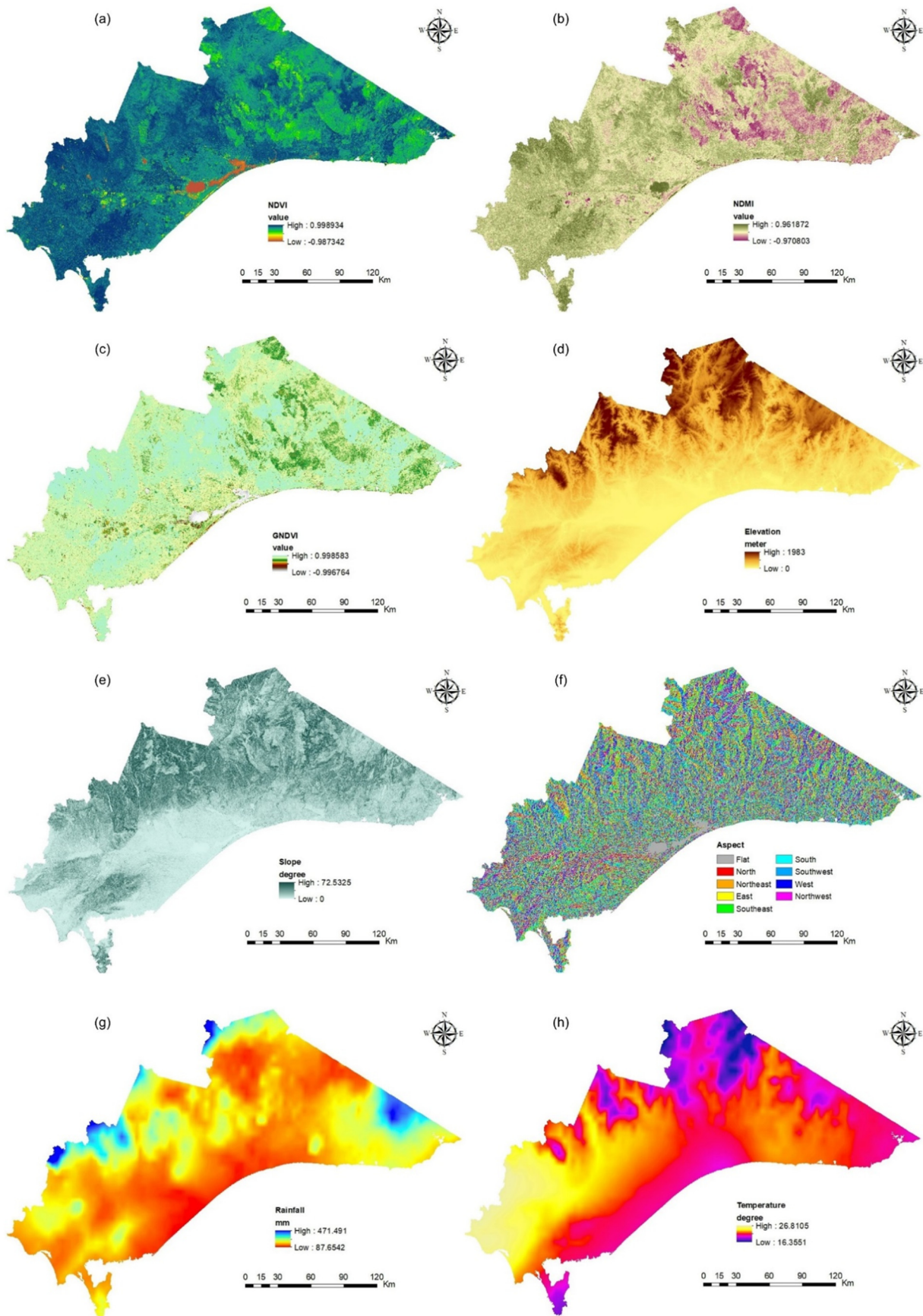


Fig. 3. Contributing variables in the modeling of forest fire susceptibility: (a) NDVI, (b) NDMI, (c) GNDVI, (d) elevation, (e) slope, (f) aspect, (g) rainfall, (h) temperature, (i) humidity, (j) wind speed, and (k) land cover.

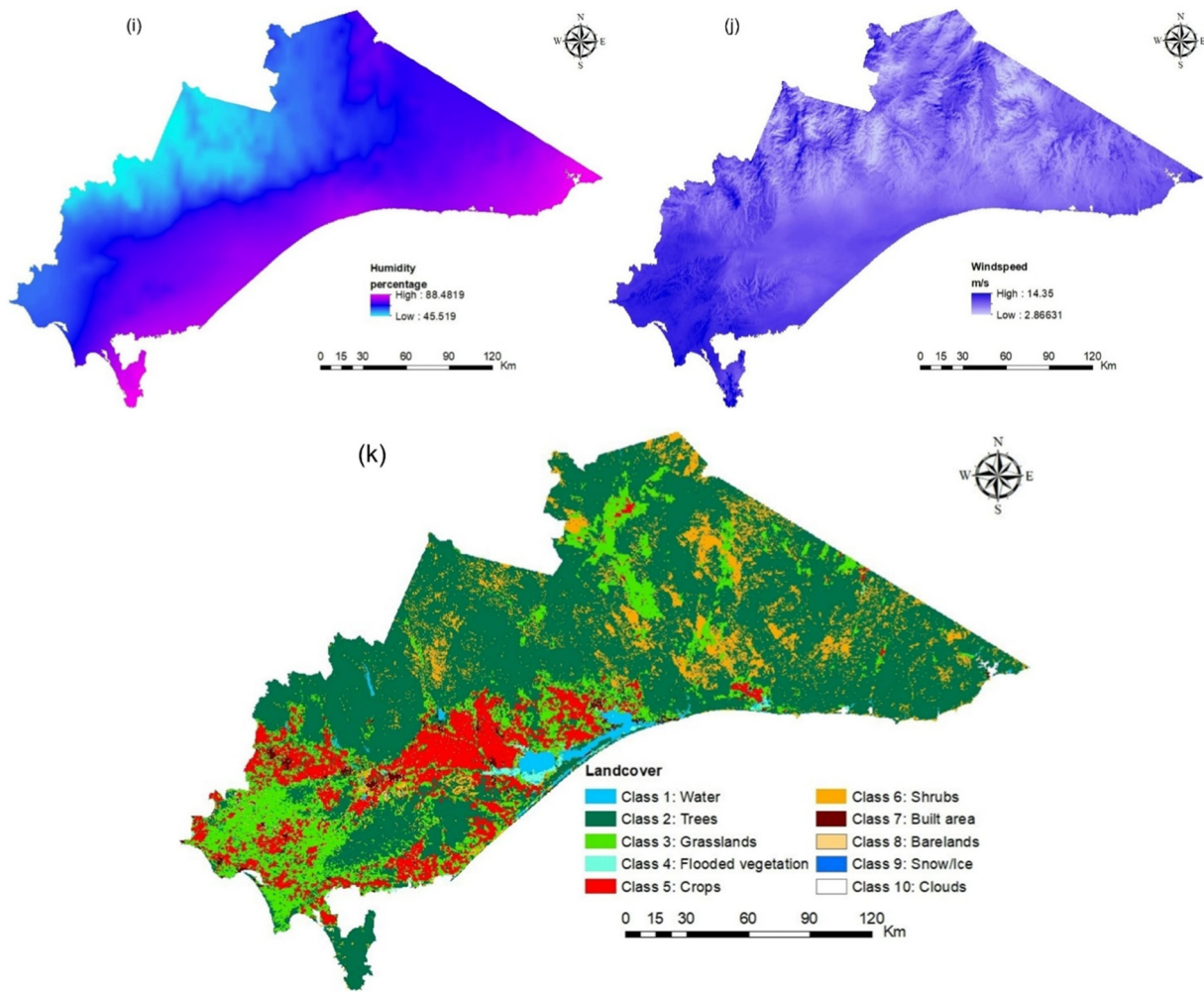


Fig. 3 (continued).

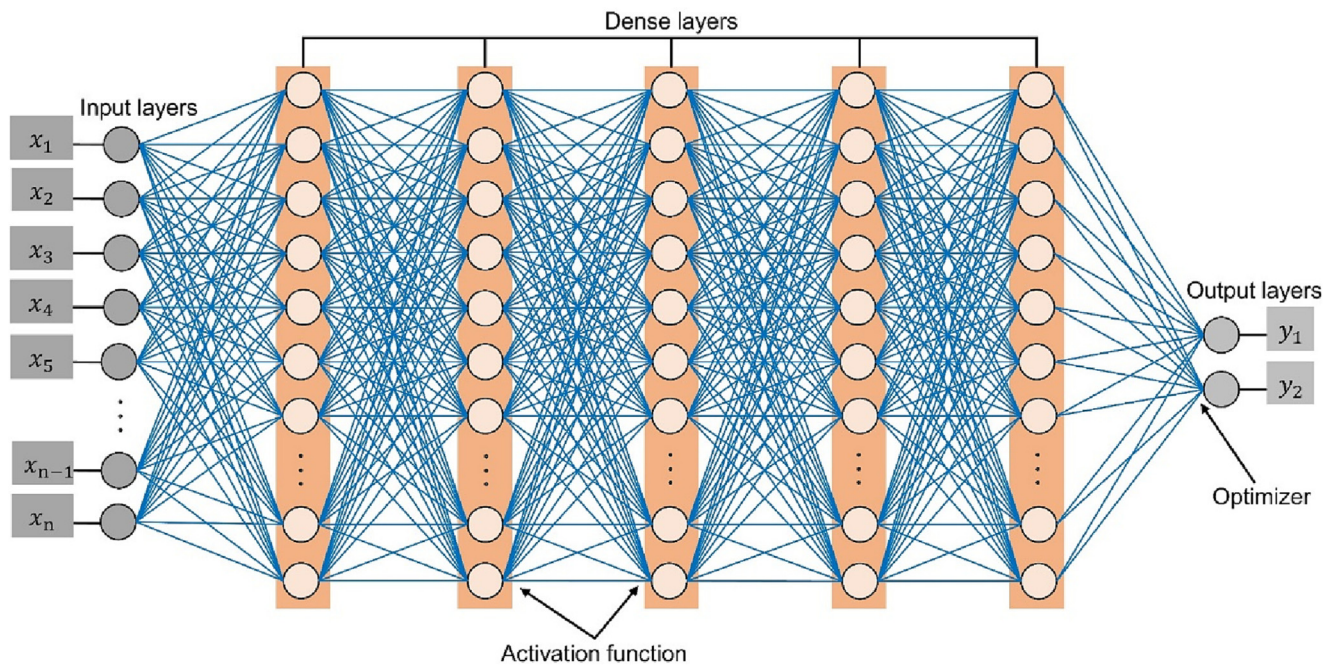
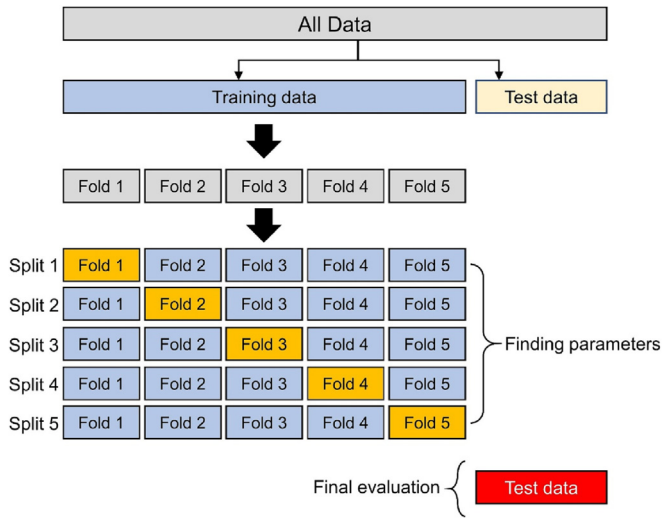


Fig. 4. The suggested DNN network's architecture for wildfire susceptibility mapping.



**Fig. 5.** Five-fold cross-validation (CV) for a more trustworthy model performance assessment. A randomly chosen fold of the inventory wildfire data is represented by each segment. The blue regions were used for training the model, whereas the orange portions were utilized for testing.

**2.5. Training and testing datasets**

Machine learning (ML) methods usually follow a typical methodology that involves training the model on a training dataset and then applying the trained method to the unseen test data to predict phenomena like wildfires. Thus, when the training and test datasets are inappropriate, ML methods produce random results that have no scientific value. A single hold-out dataset and cross-validation (CV) method is one potential strategy for a more trustworthy model performance assessment. In the optimization stage, the CV technique eliminates dataset biases and prevents the ML algorithm from being under or overfit (Tonini et al., 2020). The dataset was prepared using this process for the proposed DL models' training and testing.

**Table 2**  
The linguistic explanation of the area under the curve (AUC) values.

AUC values	Linguistic explanation
0.50–0.60	Fail
0.60–0.70	Poor
0.70–0.80	Fair
0.80–0.90	Good
0.90–1.00	Excellent

Thus, the wildfire inventory dataset *d* was randomly divided into five folds (e.g., *d*<sub>1</sub>, *d*<sub>2</sub>, *d*<sub>3</sub>, *d*<sub>4</sub>, *d*<sub>5</sub>) that were mutually exclusive, and then the proposed method ran five times. One fold was set aside for validation at any time and was not used for training. Hence, the model was trained using 80 % of the wildfire inventory data at each time, and its performance was verified using the remaining 20 % of the data. The five-fold cross-validation (CV) for our wildfire inventory dataset is shown in Fig. 5.

**2.6. Accuracy assessment**

To verify the accuracy of the suggested wildfire susceptibility model, four commonly used metrics (Naderpour et al., 2021), such as receiver operating characteristic (ROC), precision, recall, overall accuracy, and F1 score, were applied in this work. As previously noted, we employed a five-fold CV approach for a more uniform assessment of the effectiveness of the utilized DL model. In order to assess the model's performance, we looked at the consistency between the validation folds of the inventory dataset and the outputs of the utilized technique using the ROC curve approach, a popular accuracy evaluation tool. The plotted ROC curves demonstrate the trade-off between the false positive rate (FPR) on the X axis and the true positive rate (TPR) on the Y axis, where the area under the curve (AUC) can be determined by Eq. (3).

$$AUC = \sum_{i=1}^n [x_{i+1} + 1 - x_i] \times [y_i + (y_{i+1} - y_i) / 2] \tag{3}$$

where, *n* is the total number of pixels, *y<sub>i</sub>* is the percentage of correctly predicted pixels, and *x<sub>i</sub>* is the percentage of incorrectly predicted pixels (Schneider and Pontius Jr, 2001). The resulting values are explained linguistically in Table 2. AUC values close to 0 demonstrate that the prediction is random, whereas AUC values close to 1 imply high accuracy for a wildfire susceptibility map.

**3. Results of SHAP method**

We illustrated the explanations provided by the SHAP technique in this section. Typically, the influence of the features in a model is shown in a partial dependence plot, which highlights the effects of changing a single characteristic, or by a bar plot, which highlights the features' global significance (García and Aznarte, 2020). However, as SHAP values are the results of unique features that are particular to each prediction, additional types of visualizations are feasible. The expected results of a technique are displayed in the SHAP dependence graphs when the value of the characteristics is stable. Partial dependence plots can be replaced by SHAP dependence graphs since they better depict the effects of feature relationships. We can demonstrate in the dependence plots how the model is dependent on a specific feature by demonstrating how the model outputs vary as the features change.

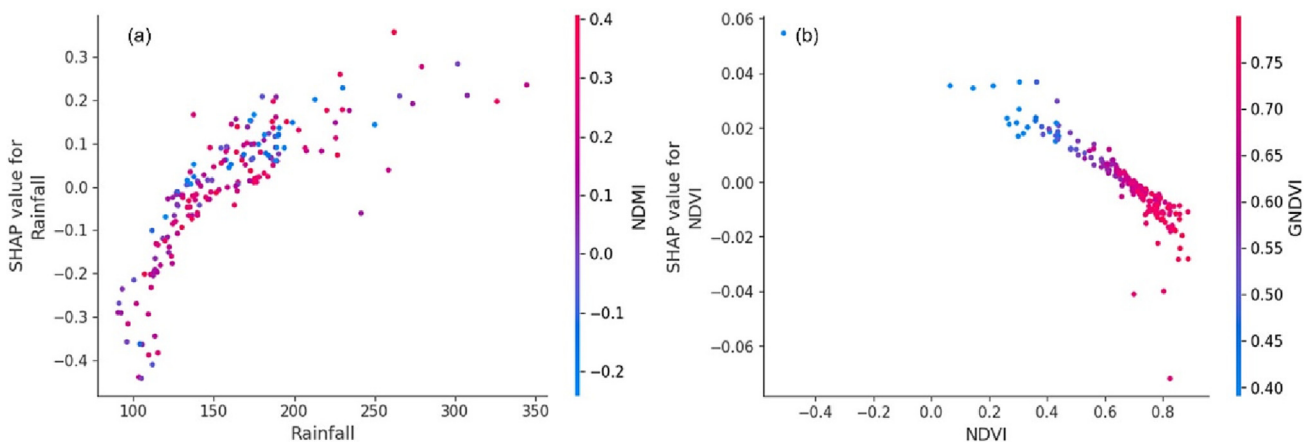


**Fig. 6.** The proposed method's SHAP dependence plots on (a) rainfall and NDMI, and (b) NDVI and GNDVI for wildfire prediction.

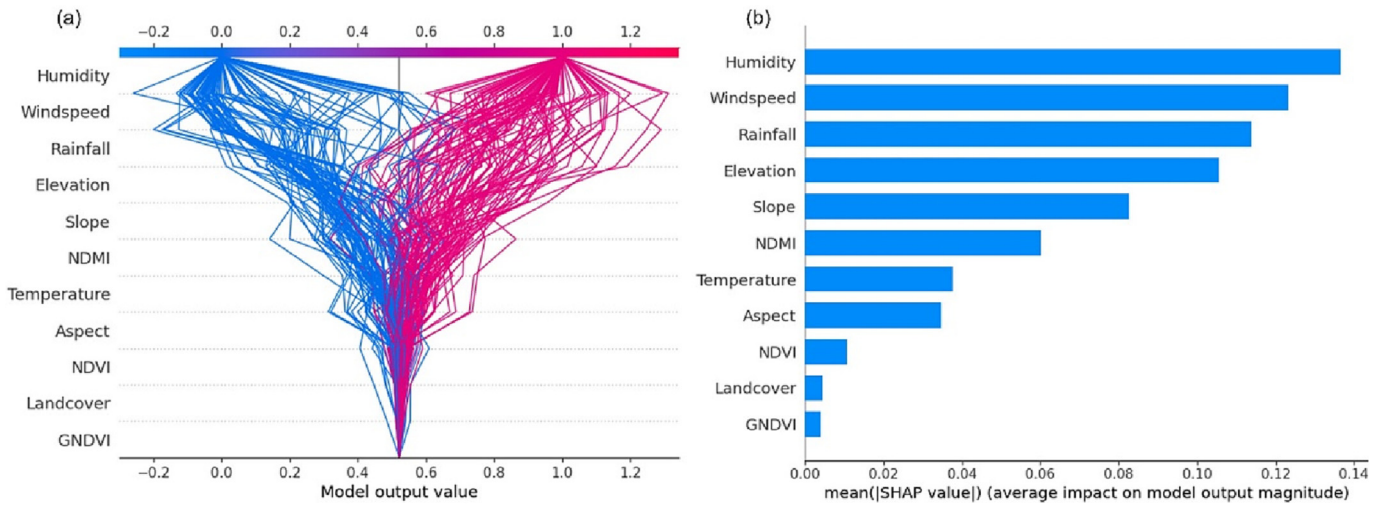


Fig. 7. A global view of contribution to prediction using: (a) decision plot; and (b) a bar graph.

For instance, to better understand factors relationships, we presented the interactions between them for the wildfire prediction based on SHAP values in Fig. 6. This is demonstrated in Fig. 6a for rainfall and NDMI, and Fig. 6b for NDVI and GNDVI, where the colors correspond to the SHAP values assigned to each variable, and the X and Y axes show their magnitudes. The influence of rainfall is shown for NDMI change from -0.2 to 0.4, and the influence of NDVI is shown for GNDVI change from 0.4 to 0.75. Red and blue are used to show the high and low values of the variable NDMI and GNDVI, respectively. In Fig. 6a, when rainfall is less than 150 mm, the SHAP values for rainfall are less than 0; low rainfall and NDMI cause the SHAP values to be incredibly low, which increases the likelihood of wildfire prediction.

In Fig. 7a, we showed the influential features in deriving the proposed model's output wildfire score prediction using a decision plot. The proposed model factors are listed on the Y axis in order of decreasing influence, while the X axis reflects the output value of the model. A line is used to depict the

prediction for each observation. At the anticipated value for the pertinent observation at the top of the figure, each line crosses the X axis. The SHAP values of each parameter are added to the base value of the model as we move from the bottom of the plot to the top. The additive values illustrate how each model factor affects the final forecast. The wildfire score is favorably influenced by variables with moving rightward lines, while it is adversely affected by variables with lines that move to the left of the plot. Additionally, we used a normal bar graph (Fig. 7b), which brings the whole data to a single plot to calculate the average absolute value of SHAP values for each feature. The magnitude of the difference in log-odds is shown by the SHAP values on the X axis. In this case, all features are continuous, and their average impact on categorization is organized vertically in the rank order, with the lowest feature contributing the least to the predictions and the top feature contributing the most. The decision plot provides a broad overview of the contribution to prediction as the bar graph. According to the decision plot and bar graph, one can see that

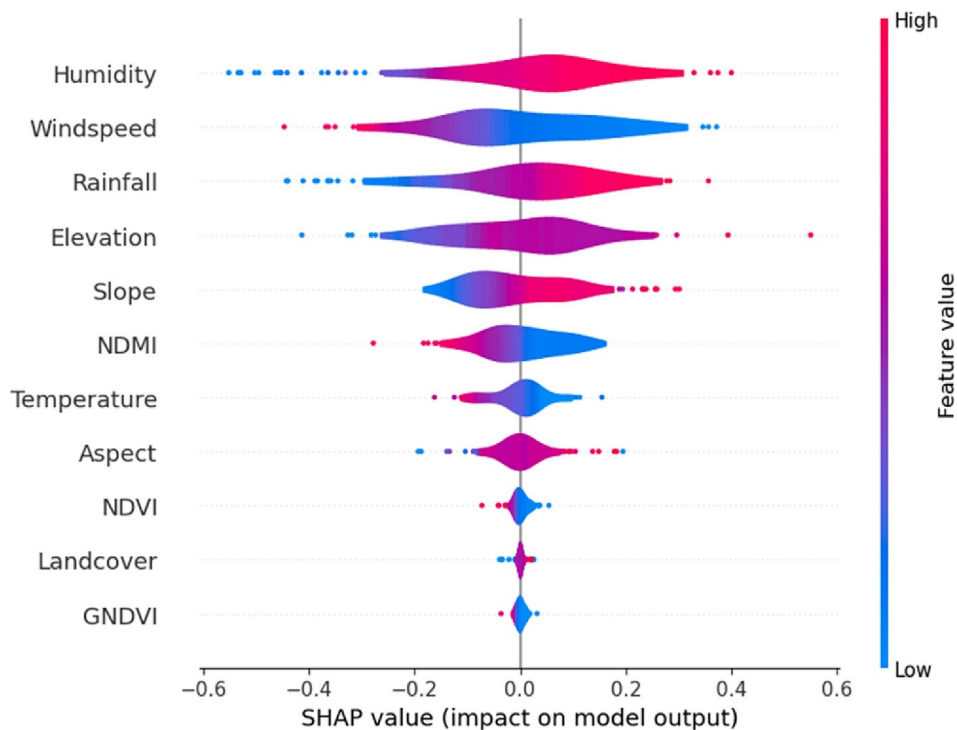


Fig. 8. The SHAP summary visualization of the proposed model. The higher SHAP value of a feature corresponds to the higher prediction.

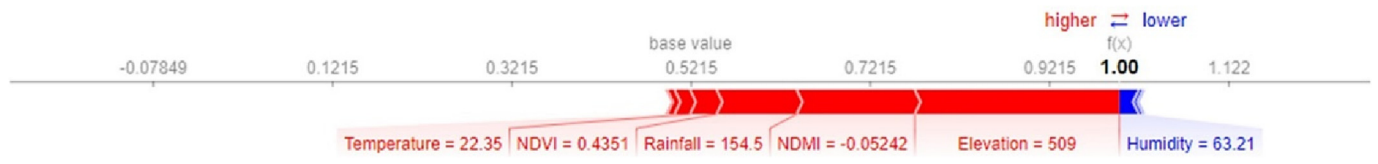


Fig. 9. Local interpretation of the proposed model's prediction using a SHAP force plot. Red feature attributions push the results higher than the "base value," whereas blue feature attributions push the outcome lower.

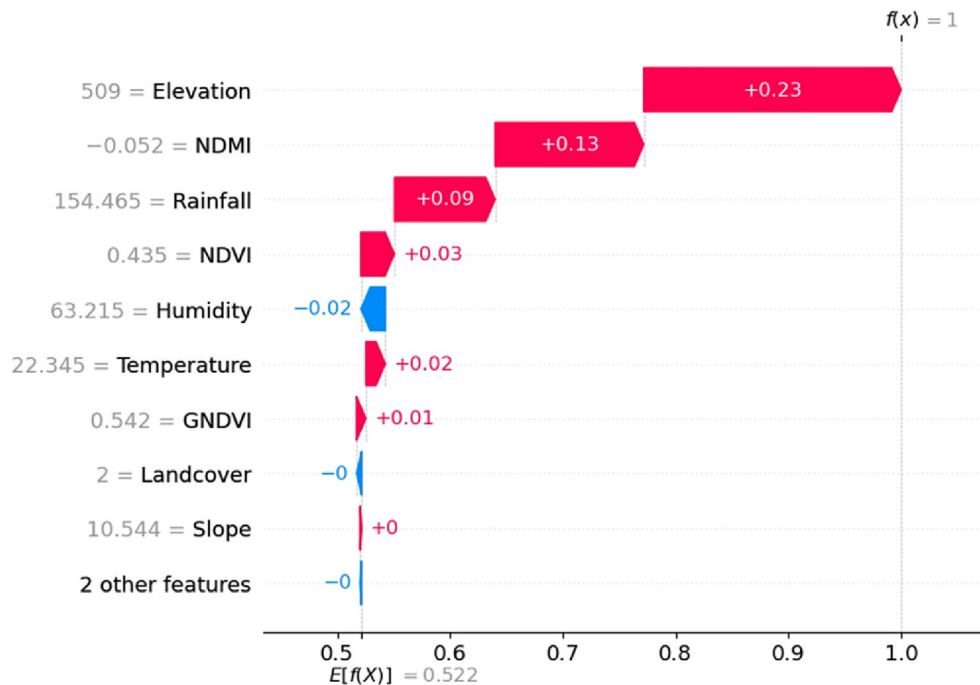


Fig. 10. Showing explanations for individual predictions using a waterfall plot. The expected value of the model output is shown at the bottom, and each row illustrates how the contribution of each feature, whether negative (blue) or positive (red), shifts the value from the expected model output to the prediction.

humidity, wind speed, rainfall, elevation, slope, and NDMI have the strongest influence on wildfire prediction.

In order to merge the importance of the feature with its effects, we also created a summary plot. Each point on the summary plot represents a Shapley value for a feature and a sample. The summary plot for the various features of the wildfire prediction is shown in Fig. 8. The features are displayed on the Y axis, and the Shapley value is determined by the X axis. The color denotes each feature's value, which ranges from low to high. The X axis indicates a positive, and the red color denotes a high value. The features are vertically ordered by their average importance on the predictions (Ribeiro et al., 2016). According to the overlapping points that are jittered in the Y axis direction, we can determine how much Shapley values dispensation there is for each feature. We can see how humidity has the greatest influence on prediction, with high values of humidity correlated with adverse effects on prediction, while the target factor and the wind speed have a positive relationship.

We utilized a force plot to show an explanation of a prediction made by the proposed model in Fig. 9. In the explanation, it is shown how several features interact to push the model's output from the "base" value to the "predicted" value. Red represents features that lead to a high prediction rating, whereas blue denotes features that lead to a lower result. For instance, the sample's forecast for the wildfire is 1.00, while the baseline value is 0.5215. The final output prediction can be enhanced by the relatively high NDVI, temperature and elevation, and low NDMI and rainfall, while the forecast can be diminished by the relatively high humidity. Fig. 10 also depicts a waterfall plot, which is designed to show explanations for individual predictions. Negative values reflect an indirect association with wildfire susceptibility, whereas positive values reflect a direct relationship

according to the model's calculations. For instance, the likelihood of fire increased when the rainfall value was lower. The magnitude weight of the variables (whether positive or negative) reveals their strong correlation with wildfire. Thus, elevation was influential to wildfire, followed by NDMI and rainfall as +0.23, +0.13, and +0.09, respectively. To put it another way, changes in the values of the aforementioned factors are highly correlated with the absence or occurrence of wildfire initiation. Slope, land cover, and aspect obtained the lowest degree of contribution, while NDVI, temperature, GNDVI, and humidity demonstrated a moderate correlation.

Table 3

Quantitative results of the proposed model for different applied folds on training and validation datasets.

Folds	Recall (%)	Precision (%)	F1 score (%)	Accuracy (%)
<i>Training scores</i>				
Fold 1	96.35	94.06	95.19	94.62
Fold 2	94.52	91.20	92.83	91.93
Fold 3	94.84	95.71	95.28	94.78
Fold 4	97.27	90.42	93.72	92.77
Fold 5	93.03	93.88	93.45	92.78
Average	95.20	93.05	94.09	93.38
<i>Validation scores</i>				
Fold 1	92.77	87.50	90.05	88.59
Fold 2	92.77	86.51	89.53	87.91
Fold 3	81.70	88.15	84.81	83.89
Fold 4	91.46	85.22	88.23	86.57
Fold 5	91.46	88.23	89.82	88.51
Average	90.03	87.12	88.49	87.09

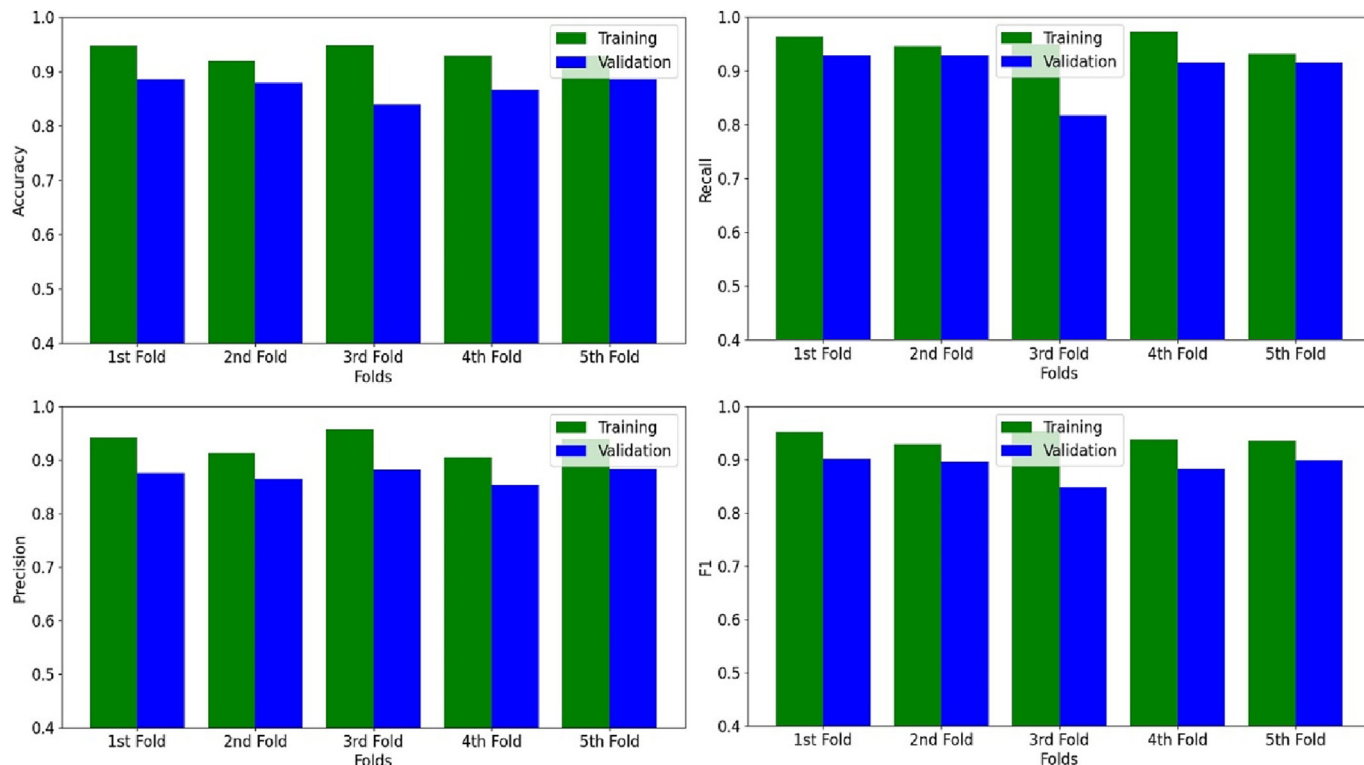


Fig. 11. Different metric's results obtained by the proposed model for different implemented folds on training and validation datasets.

4. Wildfire susceptibility prediction

As previously noted, we employed a five-fold CV procedure for a more uniform assessment of the effectiveness of the utilized DL model for wildfire susceptibility mapping. The quantitative results of different metrics (e.g., precision, recall, accuracy, and F1 score) achieved by the proposed model for all implemented folds and the average of all for training and

validation sets are shown in Table 3 and Fig. 11. We also plotted the results of ROC curves based on a five-fold CV for the test data, which is shown in Fig. 12. According to the results, the suggested technique achieved more than 93 %, and 87 % average accuracy for various metrics for all applied folds on training, and validation datasets, respectively, and mean AUC of 91 % for test dataset, which is quite substantial in this field based on the AUC values explained in Section 2.6. Additionally, the wildfire

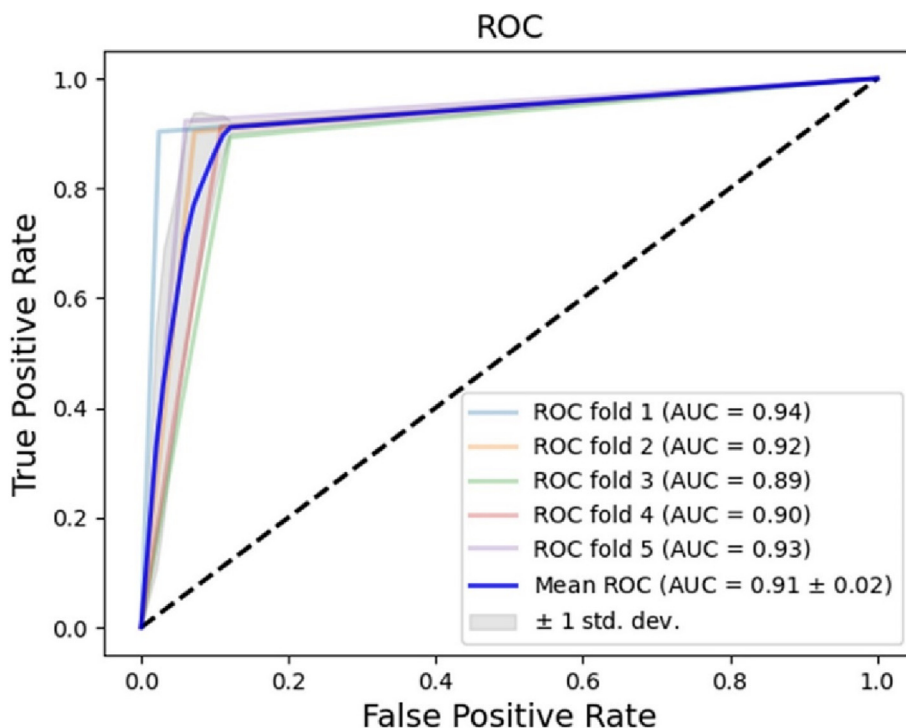


Fig. 12. The resulting ROC curve according to the five-fold cross validation on test dataset.

susceptibility map was produced based on the proposed DL approach for the study area. The resulting wildfire susceptibility prediction was divided into five classes of very-high, high, moderate, low, and very-low by the natural break algorithm, which is a standard method and designed to best groups similar values together (Febrianto et al., 2016). Fig. 13a displays the outcomes of the classification. Compared to other climate variables, the area's low rainfall and humidity rate increased the susceptibility to wildfire ignition. Due to the prevalence of forests and shrubs, suburbs such as East Gippsland and Wellington were classified as very-high/high and high/moderate wildfire susceptible zones to

as shown in Fig. 13a. This result is consistent with the results of the burned area map achieved from fire history data, which shows that most of the burned areas, including wildfire and prescribed burning, are in the East Gippsland and Wellington suburbs, as represented in Fig. 13b. The area of wildfire susceptibility prediction for each class is presented in Table 4. Generally, very low to low susceptible zones cover around 57 % of the research area, while around 33 % of the region is designated as high or very-high susceptible zones for wildfire. Approximately 9 % of the research's study region is in a moderately susceptible zone.

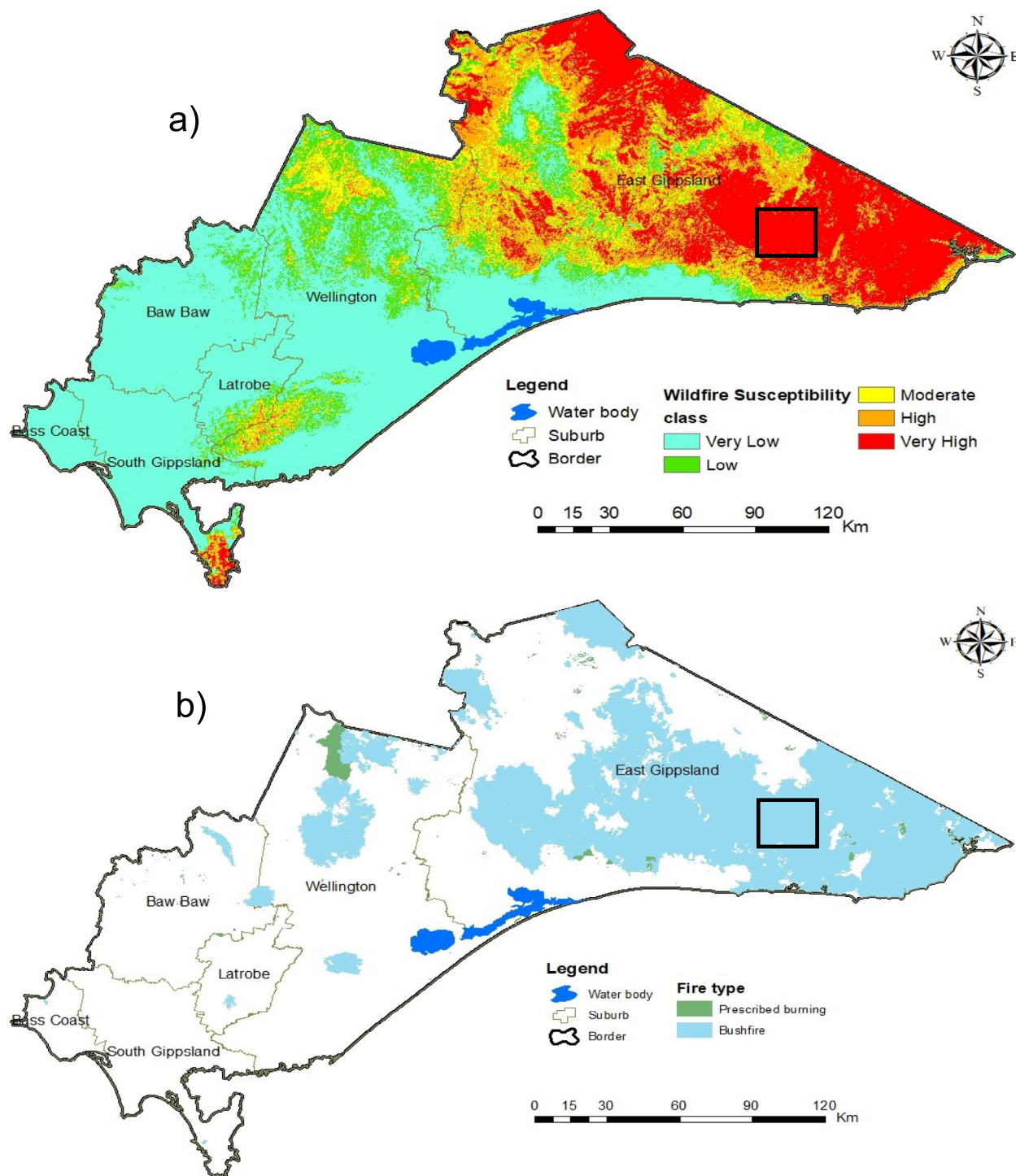


Fig. 13. (a) The wildfire susceptibility map using the proposed model; and (b) map showing the fire history burnt area.

**Table 4**

The area of each wildfire susceptibility class in the study area.

Susceptibility class	Area (km <sup>2</sup> )	Area (%)
Very low	19,196.02	45.93
Low	4902.36	11.73
Moderate	3778.29	9.04
High	5876.48	14.06
Very high	8040.21	19.23

## 5. Discussion

It's critical to recognize wildfire hazards in order to gain a better knowledge of the dynamics of wildfires in wildfire-prone locations. Because of the inherent variability of the contributing factors, creating the ideal approach for wildfire susceptibility mapping is a challenge. A literature review showed that the common machine learning (ML) algorithms such as NN, SVM, and RF or state-of-the-art DL models are suitable for modeling wildfire susceptibility (Bjånes et al., 2021; Kalantar et al., 2020; Verde and Zêzere, 2010). Studies demonstrate that ML or DL models outperform statistical techniques and knowledge-based multi-criteria decision-making for wildfire susceptibility predictions and mapping (Mohajane et al., 2021). Additionally, these techniques can be used as decision-support tools to simulate wildfires and learn more about managing their risk (Talukdar et al., 2022). However, these approaches perform differently as they cope with various input data. The performance of the ML or DL models, which is greatly influenced by the characteristics of the different input data, is directly related to the accuracy of wildfire susceptibility maps. Hence, various wildfire susceptibility maps can be produced because of the variability of each model's structure as well as conditioning factors used as input to the models. This could be a concern because these maps will be utilized by decision-makers and managers of natural resources to help them carry out corresponding environmental plans. Therefore, it is critical to assess and interpret these attributes with reference to their use in the training and testing of the models. Aside from aiming for high accuracy, understanding the reasoning behind each prediction is crucial when creating a model for wildfire susceptibility prediction.

In this work, with the use of an explainable machine learning technique, we demonstrated how to interpret the results of the developed model for wildfire susceptibility prediction and identify the variables influencing the prediction model for the Gippsland region in Victoria, Australia. Each characteristic of every data point is given a SHAP value by the approach, which serves as a contribution value for the model's result. Using these SHAP values, we encoded and arranged the features according to their relevance using every feature's contribution information. In this case, selecting a group of features based on the SHAP values necessitates sorting the features according to how much they contribute to the output of the model. Using the SHAP values assigned to each feature and the interpretation of how the features affect the prediction in Section 3, we found that contributing factors such humidity, wind speed and rainfall from meteorological factors, elevation and slope from topographical factors, and NDMI from land cover/vegetation factors demonstrated a significant impact and high contribution on the suggested model's output for wildfire susceptibility prediction. Wind not only carries fire flames and sparks into fresh vegetation, but also removes soil/surface moisture. The surface fuels can also be more susceptible to fire ignition in the presence of lower rainfall, humidity, and warmer temperatures. Elevation and slope control the climate, especially how temperature and rainfall are distributed spatially. Additionally, the NDMI employs short-wave infrared (SWIR) bands, where a low value of it will significantly impact the occurrence of wildfires due to its sensitivity to vegetation density, moisture, and forest structure (Schroeder et al., 2011). The development of an efficient and reliable framework, such as the explainable artificial intelligence model (XAI) used in this study, along with the interpretation of different SHAP plots, will assist decision-makers in better understanding the model's outputs and identifying which parameters are showing high contributions and having an impact on the

wildfire prediction model, and as a result, will help them better control the risk of fires. While Explainable AI (XAI) has the potential to address many of the limitations of traditional black-box AI models, it also has its own set of limitations such as complexity. Developing an XAI model that is both accurate and interpretable can be challenging. As a result, many XAI models may sacrifice accuracy in order to improve interpretability, or vice versa. Also, XAI models rely on the availability of high-quality data in order to be effective. If there is limited or low-quality data available, XAI models may be less accurate or less interpretable.

## 6. Conclusion

An essential component of land emergency management, reducing the effects of natural disasters, and facilitating the response and recovery of firefighters is the spatial evaluation of wildfire hazards in wildfire-prone areas, which poses a threat to property and human life. Based on the capabilities of the explainable machine learning model, this paper developed a framework for wildfire susceptibility assessment in the Gippsland region in Victoria, Australia. Several contributing factors from three categories (e.g., meteorological, topographic, and land cover/vegetation factors) were fed into the model to assess their correlation with the wildfire susceptibility prediction in the study area. An explanation model called SHAP was applied to analyze the feature importance and interpret the results of the proposed model created for wildfire susceptibility prediction. We applied the SHAP technique to better understand why a data-driven approach makes any prediction on the basis of certain input data. By assigning SHAP values to each feature that contributes to the model's output, we used the SHAP technique to choose the best features influencing the prediction model. We discovered that contributing factors such as elevation and slope from topographical factors, NDMI from land cover/vegetation factors, and humidity, wind speed, and rainfall from meteorological factors indicated major effects and high contributions to wildfire susceptibility prediction. This was based on interpreting the proposed model's output using different SHAP plots. The results of this study demonstrated the applicability of the SHAP approach for interpreting the machine learning technique and its predictions. To sum up, SHAP enables thorough data analysis and guides us in choosing the proper conditioning factors and AI models for wildfire susceptibility mapping.

## Funding

This research is supported by the Fenner School of Environment & Society, College of Science, Australian National University (ANU), and the Centre for Advanced Modelling and Geospatial Information Systems (CAMGIS), Faculty of Engineering and IT, the University of Technology Sydney (UTS).

## CRediT authorship contribution statement

**Abolfazl Abdollahi:** Conceptualization, Methodology, Formal analysis, Data curation, Writing – original draft. **Biswajeet Pradhan:** Writing – review & editing, Supervision, Funding acquisition.

## Data availability

Data will be made available on request.

## Declaration of competing interest

The authors declare no conflict of interest.

## References

- Abdollahi, A., Liu, Y., Pradhan, B., Huete, A., Dikshit, A., Tran, N.N., 2022. Short-time-series grassland mapping using Sentinel-2 imagery and deep learning-based architecture. *Egypt. J. Remote Sens. Space Sci.* 25, 673–685.
- Abdollahi, A., Pradhan, B., 2021. Urban vegetation mapping from aerial imagery using explainable AI (XAI). *Sensors* 21, 4738.

- Adab, H., Kanniah, K.D., Solaimani, K., 2013. Modeling forest fire risk in the northeast of Iran using remote sensing and GIS techniques. *Nat. Hazards* 65, 1723–1743.
- Ajin, R., Ciobotaru, A.-M., Vinod, P., Jacob, M.K., 2015. Forest and wildland fire risk assessment using geospatial techniques: a case study of Nemmara forest division, Kerala, India. *J. Wetl. Biodivers.* 5, 29–37.
- Al-Fugara, A.K., Mabdeh, A.N., Ahmadlou, M., Pourghasemi, H.R., Al-Adamat, R., Pradhan, B., et al., 2021. Wildland fire susceptibility mapping using support vector regression and adaptive neuro-fuzzy inference system-based whale optimization algorithm and simulated annealing. *ISPRS Int. J. Geo Inf.* 10, 382.
- Arrieta, A.B., Díaz-Rodríguez, N., Del Ser, J., Bennetot, A., Tabik, S., Barbedo, A., et al., 2020. Explainable artificial intelligence (XAI): concepts, taxonomies, opportunities and challenges toward responsible AI. *Inf. Fusion* 58, 82–115.
- Bjånes, A., De La Fuente, R., Mena, P., 2021. A deep learning ensemble model for wildfire susceptibility mapping. *Eco. Inform.* 65, 101397.
- Chen, S., 2021. Interpretation of Multi-label Classification Models Using Shapley Values, pp. 1–12. <https://arxiv.org/abs/2104.10505>.
- Cheng, X., Wang, J., Li, H., Zhang, Y., Wu, L., Liu, Y., 2021. A method to evaluate task-specific importance of spatio-temporal units based on explainable artificial intelligence. *Int. J. Geogr. Inf. Sci.* 35, 2002–2025.
- Chuvieco, E., Allgöwer, B., Salas, J., 2003. Integration of physical and human factors in fire danger assessment. *Wildland fire danger estimation and mapping: The role of remote sensing data.* World Scientific, pp. 197–218.
- Cilli, R., Elia, M., D'Este, M., Giannico, V., Amoroso, N., Lombardi, A., et al., 2022. Explainable artificial intelligence (XAI) detects wildfire occurrence in the Mediterranean countries of southern Europe. *Sci. Rep.* 12, 16349.
- Dutta, R., Das, A., Aryal, J., 2016. Big data integration shows australian bush-fire frequency is increasing significantly. *R. Soc. Open Sci.* 3, 150241.
- Eskandari, S., Khoshnevis, M., 2020. Evaluating and mapping the fire risk in the forests and rangelands of sirachal using fuzzy analytic hierarchy process and GIS. *For. Res. Dev.* 6, 219–245.
- Eskandari, S., Miesel, J.R., 2017. Comparison of the fuzzy AHP method, the spatial correlation method, and the dong model to predict the fire high-risk areas in hyrcanian forests of Iran. *Geomat. Nat. Haz. Risk* 8, 933–949.
- Eskandari, S., Pourghasemi, H.R., Tiefenbacher, J.P., 2021. Fire-susceptibility mapping in the natural areas of Iran using new and ensemble data-mining models. *Environ. Sci. Pollut. Res.* 28, 47395–47406.
- Febrianto, H., Fariza, A., Hasim, J.A.N., 2016. Urban flood risk mapping using analytic hierarchy process and natural break classification (Case study: Surabaya, East Java, Indonesia). 2016 International Conference on Knowledge Creation and Intelligent Computing (KIC). *IEEE*, pp. 148–154.
- Ganteaume, A., Camia, A., Jappiot, M., San-Miguel-Ayanz, J., Long-Fournel, M., Lampin, C., 2013. A review of the main driving factors of forest fire ignition over Europe. *Environ. Manag.* 51, 651–662.
- García, M.V., Aznarte, J.L., 2020. Shapley additive explanations for NO2 forecasting. *Eco. Inform.* 56, 101039.
- Gholamnia, K., Gudiyangada Nachappa, T., Ghorbanzadeh, O., Blaschke, T., 2020. Comparisons of diverse machine learning approaches for wildfire susceptibility mapping. *Symmetry* 12, 604.
- Glorot, X., Bordes, A., Bengio, Y., 2011. Deep sparse rectifier neural networks. *Proceedings of the fourteenth international conference on artificial intelligence and statistics. JMLR Workshop and Conference Proceedings*, pp. 315–323.
- González, C., Castillo, M., García-Chevesich, P., Barrios, J., 2018. Dempster-Shafer theory of evidence: a new approach to spatially model wildfire risk potential in Central Chile. *Sci. Total Environ.* 613, 1024–1030.
- Iban, M.C., Sekertekin, A., 2022. Machine learning based wildfire susceptibility mapping using remotely sensed fire data and GIS: a case study of Adana and Mersin provinces, Turkey. *Eco. Inform.* 69, 101647.
- Jaafari, A., Pourghasemi, H.R., 2019. Factors influencing regional-scale wildfire probability in Iran: an application of random forest and support vector machine. *Spatial modeling in GIS and R for Earth and Environmental Sciences.* Elsevier, pp. 607–619.
- Jaafari, A., Zenner, E.K., Panahi, M., Shahabi, H., 2019. Hybrid artificial intelligence models based on a neuro-fuzzy system and metaheuristic optimization algorithms for spatial prediction of wildfire probability. *Agric. For. Meteorol.* 266, 198–207.
- Jaiswal, R.K., Mukherjee, S., Raju, K.D., Saxena, R., 2002. Forest fire risk zone mapping from satellite imagery and GIS. *Int. J. Appl. Earth Obs. Geoinf.* 4, 1–10.
- Kalantar, B., Ueda, N., Idrees, M.O., Janizadeh, S., Ahmadi, K., Shabani, F., 2020. Forest fire susceptibility prediction based on machine learning models with resampling algorithms on remote sensing data. *Remote Sens.* 12, 3682.
- Kim, S.J., Lim, C.-H., Kim, G.S., Lee, J., Geiger, T., Rahmati, O., et al., 2019. Multi-temporal analysis of forest fire probability using socio-economic and environmental variables. *Remote Sens.* 11, 86.
- Kuter, N., Yenilmez, F., Kuter, S., 2011. Forest fire risk mapping by kernel density estimation. *Croat. J. For. Eng.* 32, 599–610.
- Ljubomir, G., Pamučar, D., Drobňjak, S., Pourghasemi, H.R., 2019. Modeling the spatial variability of forest fire susceptibility using geographical information systems and the analytical hierarchy process. *Spatial modeling in GIS and R for Earth and Environmental Sciences.* Elsevier, pp. 337–369.
- Lundberg, S., Lee, S.-I., 2017. A Unified Approach to Interpreting Model Predictions, pp. 1–10. <https://arxiv.org/abs/1705.07874>.
- Maddy, E.S., Boukabara, S.A., 2021. MIIDAPS-AI: an explainable machine-learning algorithm for infrared and microwave remote sensing and data assimilation preprocessing-application to LEO and GEO sensors. *IEEE J. Sel. Top. Appl. Earth Obs. Remote Sens.* 14, 8566–8576.
- Mangalathu, S., Hwang, S.-H., Jeon, J.-S., 2020. Failure mode and effects analysis of RC members based on machine-learning-based SHapley additive exPlanations (SHAP) approach. *Eng. Struct.* 219, 110927.
- Mohajane, M., Costache, R., Karimi, F., Pham, Q.B., Essahlaoui, A., Nguyen, H., et al., 2021. Application of remote sensing and machine learning algorithms for forest fire mapping in a Mediterranean area. *Ecol. Indic.* 129, 107869.
- Molina, J.R., González-Cabán, A., y Silva, F.R., 2019. Wildfires impact on the economic susceptibility of recreation activities: application in a Mediterranean protected area. *J. Environ. Manag.* 245, 454–463.
- Naderpour, M., Rizeei, H.M., Ramezani, F., 2021. Forest fire risk prediction: a spatial deep neural network-based framework. *Remote Sens.* 13, 2513.
- Nami, M., Jaafari, A., Fallah, M., Nabiuni, S., 2018. Spatial prediction of wildfire probability in the hyrcanian ecoregion using evidential belief function model and GIS. *Int. J. Environ. Sci. Technol.* 15, 373–384.
- Navarro, G., Caballero, I., Silva, G., Parra, P.-C., Vázquez, Á., Caldeira, R., 2017. Evaluation of forest fire on Madeira Island using sentinel-2A MSI imagery. *Int. J. Appl. Earth Obs. Geoinf.* 58, 97–106.
- Pradhan, B., Suliman, M.D.H.B., Awang, M.A.B., 2007. Forest fire susceptibility and risk mapping using remote sensing and geographical information systems (GIS). *Disaster Prev Manag.* 16 (3), 344–352.
- Ribeiro, M.T., Singh, S., Guestrin, C., 2016. "Why should I trust you?" Explaining the predictions of any classifier. *Proceedings of the 22nd ACM SIGKDD International Conference on Knowledge Discovery and Data Mining*, pp. 1135–1144.
- Sayad, Y.O., Mousannif, H., Al Moatassime, H., 2019. Predictive modeling of wildfires: a new dataset and machine learning approach. *Fire Saf. J.* 104, 130–146.
- Schneider, L.C., Pontius Jr., R.G., 2001. Modeling land-use change in the Ipswich watershed, Massachusetts, USA. *Agric. Ecosyst. Environ.* 85, 83–94.
- Schroeder, T.A., Wulder, M.A., Healey, S.P., Moisen, G.G., 2011. Mapping wildfire and clearcut harvest disturbances in boreal forests with landsat time series data. *Remote Sens. Environ.* 115, 1421–1433.
- Shakesby, R., 2011. Post-wildfire soil erosion in the Mediterranean: review and future research directions. *Earth Sci. Rev.* 105, 71–100.
- Shrikumar, A., Greenside, P., Kundaje, A., 2017. Learning important features through propagating activation differences. *International Conference on Machine Learning. PMLR*, pp. 3145–3153.
- Smith, J.K., Lyon, L.J., 2000. *Wildland Fire in Ecosystems: Effects of Fire on Fauna. Vol 2.* US Department of Agriculture, Forest Service, Rocky Mountain Research Station.
- Talukdar, S., Das, T., Naikoo, M.W., Rihan, M., Rahman, A., 2022. Forest fire susceptibility mapping by integrating remote sensing and machine learning algorithms. *Adv. Remote Sens. For. Monit.* 179–195.
- Tavakkoli Piralilou, S., Einali, G., Ghorbanzadeh, O., Nachappa, T.G., Gholamnia, K., Blaschke, T., et al., 2022. A Google earth engine approach for wildfire susceptibility prediction fusion with remote sensing data of different spatial resolutions. *Remote Sens.* 14, 672.
- Tien Bui, D., Le, K.-T.T., Nguyen, V.C., Le, H.D., Revhaug, I., 2016. Tropical forest fire susceptibility mapping at the cat Ba National Park Area, hai Phong City, Vietnam, using GIS-based kernel logistic regression. *Remote Sens.* 8, 347.
- Tonini, M., D'Andrea, M., Biondi, G., Degli Esposti, S., Trucchia, A., Fiorucci, P., 2020. A machine learning-based approach for wildfire susceptibility mapping. The case study of the Liguria region in Italy. *Geosciences* 10, 105.
- Vasilakos, C., Kalabokidis, K., Hatzopoulos, J., Matsinos, I., 2009. Identifying wildland fire ignition factors through sensitivity analysis of a neural network. *Nat. Hazards* 50, 125–143.
- Verde, J., Zézeze, J., 2010. Assessment and validation of wildfire susceptibility and hazard in Portugal. *Nat. Hazards Earth Syst. Sci.* 10, 485–497.
- Won, M.-S., Koo, K.-S., Lee, M.-B., 2006. An analysis of forest fire occurrence hazards by changing temperature and humidity of ten-day intervals for 30 years in spring. *Korean J. Agric. For. Meteorol.* 8, 250–259.
- Zhongming, Z., Linong, L., Xiaona, Y., Wangqiang, Z., Wei, L., 2020. *The State of the World's Forests: Forests, Biodiversity and People.* FAO, Rome, Italy.